Crustal strain partitioning and the associated earthquake hazard in the eastern Sunda-Banda Arc

Article *in* Geophysical Research Letters · February 2016
DOI: 10.1002/2016GL067941

CITATIONS
9

9 authors, including:

Susilo Susilo
Badan Informasi Geospasial
28 PUBLICATIONS **49** CITATIONS
SEE PROFILE

Simon Mcclusky
Australian National University
112 PUBLICATIONS **7,493** CITATIONS
SEE PROFILE

Irwan Meilano
Bandung Institute of Technology
128 PUBLICATIONS **741** CITATIONS
SEE PROFILE

Phil R. Cummins
Australian National University
139 PUBLICATIONS **1,987** CITATIONS
SEE PROFILE

AGU PUBLICATIONS

Geophysical Research Letters

RESEARCH LETTER
10.1002/2016GL067941

Key Points:
- The Sunda-Banda back-arc thrust system is a large active plate boundary that extends over 2000 km
- Strain is transferred from Java subduction to the back-arc thrusts via a left-lateral strike slip
- Geodetic strain across the Sunda-Banda back-arc thrusts emphasize a high seismic and tsunami hazard

Supporting Information:
- Text S1, Tables S1 and S2, and Figures S1–S9
- Data Set S1

Correspondence to:
A. Koulali,
achraf.koulali@anu.edu.au

Citation:
Koulali, A., S. Susilo, S. McClusky, I. Meilano, P. Cummins, P. Tregoning, G. Lister, J. Efendi, and M. A. Syafi'i (2016), Crustal strain partitioning and the associated earthquake hazard in the eastern Sunda-Banda Arc, *Geophys. Res. Lett.*, *43*, 1943–1949, doi:10.1002/2016GL067941.

Received 24 JAN 2016
Accepted 18 FEB 2016
Accepted article online 19 FEB 2016
Published online 11 MAR 2016

Crustal strain partitioning and the associated earthquake hazard in the eastern Sunda-Banda Arc

A. Koulali[1], S. Susilo[2], S. McClusky[1], I. Meilano[3], P. Cummins[1], P. Tregoning[1], G. Lister[1], J. Efendi[2], and M. A. Syafi'i[2]

[1]Research School of Earth Sciences, Australian National University, Canberra, Australian Capital Territory, Australia, [2]Bandan Informasi Geospatial, Cibinong, Indonesia, [3]Institute of Technology Bandung, Bandung, Indonesia

Abstract We use Global Positioning System (GPS) measurements of surface deformation to show that the convergence between the Australian Plate and Sunda Block in eastern Indonesia is partitioned between the megathrust and a continuous zone of back-arc thrusting extending 2000 km from east Java to north of Timor. Although deformation in this back-arc region has been reported previously, its extent and the mechanism of convergence partitioning have hitherto been conjectural. GPS observations establish that partitioning occurs via a combination of anticlockwise rotation of an arc segment called the Sumba Block, and left-lateral movement along a major NE-SW strike-slip fault west of Timor. We also identify a westward extension of the back-arc thrust for 300 km onshore into East Java, accommodating slip of ~6 mm/yr. These results highlight a major new seismic threat for East Java and draw attention to the pronounced seismic and tsunami threat to Bali, Lombok, Nusa Tenggara, and other coasts along the Flores Sea.

1. Introduction

Eastern Indonesia encompasses a complex tectonic environment, involving the convergence of four major tectonic Plates: the Australian, Pacific, Philippine Sea Plates, and the Sunda Block [*Hamilton*, 1979] (Figure 1). In this region the Australian Plate subducts northward beneath eastern Java, Nusa Tenggara (114°E–125°E), and the Banda Arc (Figure 1). These three arc segments accommodate a transition in the style of plate convergence from ocean-continent subduction in east Java, to arc-continent collision in Nusa Tenggara and then to the island arc subduction in the Banda Sea. While historical earthquake observations for this region are poorly known, at least seven large earthquakes have occurred between 1648 and 1891 [*Soloviev and Go*, 1974; *Musson*, 2012]. Six of these events were associated with macroseismic intensities of IX–X and four generated regional tsunamis in the Flores Sea with estimated runup of 3 m or greater [*Soloviev and Go*, 1974]. During the instrumental seismic period, four major events were reported in the area between 112°E and 128°E [*Ekström et al.*, 2012] (Figure 1). The M_w 7.9 1992 Flores earthquake was the largest thrust event recorded and generated a large, destructive tsunami [*Beckers and Lay*, 1995]. The majority of earthquakes during the last century are attributed to the back-arc segments of Flores and Wetar and have thrust style focal mechanisms [*Ekström et al.*, 2012; *Beckers and Lay*, 1995], suggesting that this fault system is accommodating an important part of the convergence between the Australian Plate and the Sunda Block.

Marine geophysical surveys [*Silver et al.*, 1983] have revealed evidence for two major back-arc thrusts: the 450 km long Flores thrust north of Sumbawa and western Flores, and the 350 km long Wetar thrust north of Timor (Figure 1). It has been speculated [*Silver et al.*, 1983] that the thick crust beneath Sumba and Timor, respectively, facilitates transfer of stress from the fore-arc to the back-arc, while the thinner crust elsewhere (e.g., Savu basin) enables convergence to be partitioned onto fore-arc and back-arc thrusts and strike-slip faults that cut the arc at angles oblique to the convergence [*McCaffrey*, 1988]. However, until now, there has been no conclusive evidence identifying which if any of these faults are facilitating the transfer of convergence.

Early geodetic investigations [*Genrich et al.*, 1996] concluded that the Timor Trough is inactive and most of the convergence between Australia, Sundaland, and Eurasia occurs to the north at a rate of 50 mm/yr. In contrast, later studies [*Bock et al.*, 2003; *Nugroho et al.*, 2009] estimated 15 to 20 mm/yr of motion across the Timor

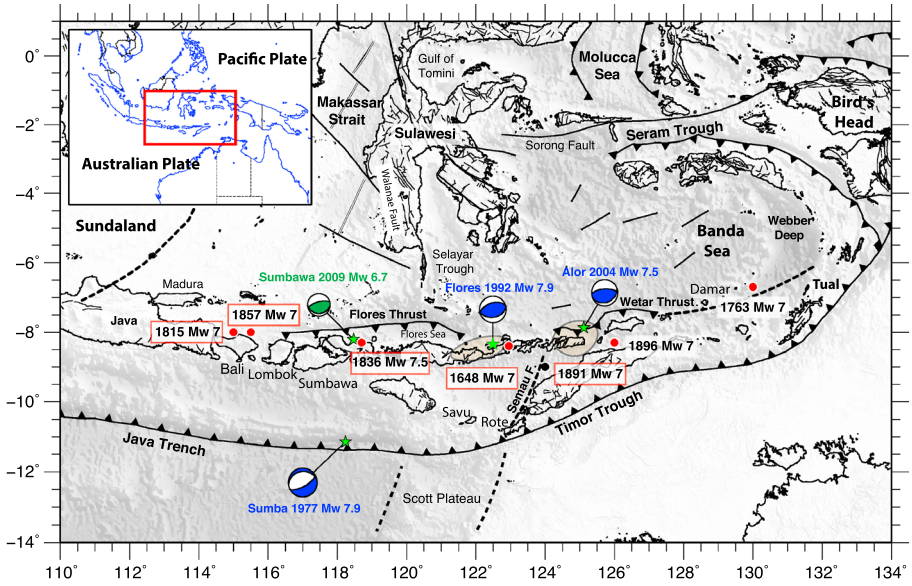

Figure 1. Seismotectonic setting of the Sunda-Banda arc-continent collision, East Indonesia. Major faults (thick black lines) [*Hamilton*, 1979]. Topography and bathymetry are from Shuttle Radar Topography Mission (http://topex.ucsd.edu/www_html/srtm30_plus.html). Focal mechanisms are from the Global Centroid Moment Tensor. Blue mechanisms correspond to earthquakes with M_w>7 (brown transparent ellipses are the corresponding rupture areas for Flores 1992 and Alor 2004 earthquakes), while the green focal mechanism shows the highest magnitude recorded in Sumbawa. Red dots indicate the locations of major historical earthquakes [*Musson*, 2012].

Trough and 60 mm/yr of shortening across the Flores Sea. The discrepancies in these results reflect the degree of uncertainty in understanding and assigning slip partitioning, mainly due to the lack of observations in the vicinity of the back-arc fault system. In addition, the lack of long and adequately sampled GPS time series makes it difficult to recognize and correct for the effects of postseismic relaxation resulting from both nearby local and regional earthquakes that have occurred since GPS observations began in the 1990s. Thus, there are many important but hitherto unanswered questions regarding the southern margin of eastern Indonesia: Is the present-day back-arc deformation localized on the Flores and Wetar segments? How does the partitioning of convergence between the subduction megathrust and back-arc vary along the Sunda-Banda Arc transition? By what mechanism does this partitioning of convergence occur? Answering these questions is essential for understanding the associated seismic and tsunami hazard. In this study, we use GPS velocities plus earthquake slip vectors to quantify slip partitioning in eastern Indonesia (110°E to 135°E) and we discuss the implications of strain distribution for earthquakes hazard in the region.

2. Methods

2.1. GPS Data Processing

The GPS velocity field presented in this study (supporting information Data Set S1) is calculated from observations at 94 GPS stations located in east Indonesia in combination with a global network of 80 International Global Navigation Satellite Systems Service tracking sites. Campaign GPS sites have been surveyed irregularly from 1993 to 2014, while most of the continuous sites operated from 2009 to 2014 (supporting information Figure S3). The raw data were processed using GAMIT-GLOBK software [*Herring et al.*, 2010], and uncertainties were estimated following standard procedures described by *Reilinger and et al.* [2006]. The velocities used in Figure 2 are with respect to a Sunda Block-fixed reference frame, defined using the velocity of only three continuous sites: BINT, NTUS, and GETI, for the period prior to the Sumatra-Andaman 2004 M_w 9.2 earthquake [*Vigny et al.*, 2005]. This approach eliminates the effects of contamination of the Sunda reference frame by postseismic effects resulting from the 2004–2012 Sumatra earthquake sequence *Feng et al.* [2015]. The weighted root-mean-square for the north and east horizontal velocity components are 0.66 mm/yr and 0.97 mm/yr, respectively, and 1.2 mm/yr for the vertical rate. For our modeling, we use only horizontal velocities and we do not include any vertical rate estimates since they have large uncertainties due to different source of systematic errors, making their usage of less importance for our block model inversions.

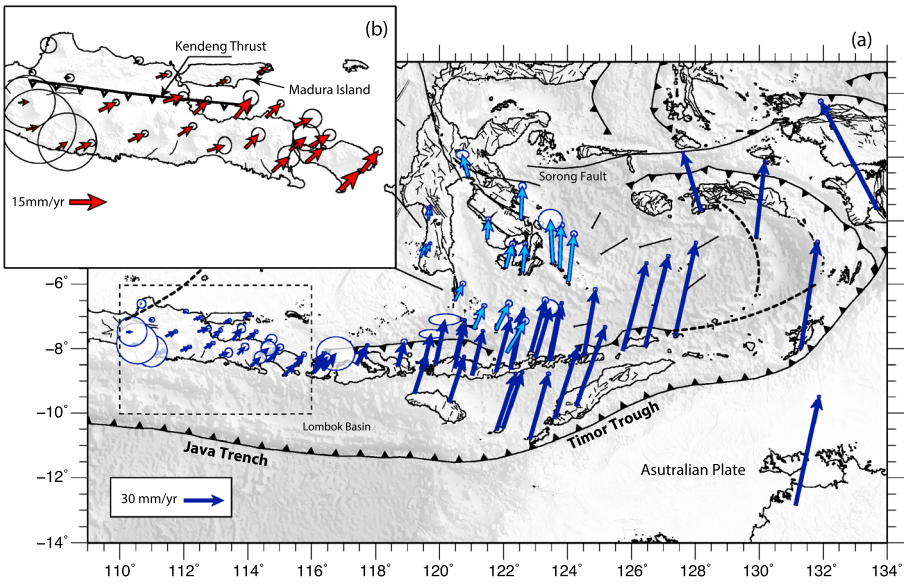

Figure 2. GPS velocities determined in this study with respect to Sunda Block. Uncertainty ellipses represent 95% confidence level. The inset figure corresponds to the area of the dashed rectangle in the map. Light blue arrows show the velocities for East and West Makassar Blocks.

2.2. Kinematic Block Modeling

We model the observed velocities as a sum of block rotations and elastic strain produced by fault locking [*McCaffrey*, 2005]. We chose block boundaries based on our qualitative interpretation of the GPS velocities themselves as well as independent information from earthquakes [*Ekström et al.*, 2012; *Shulgin et al.*, 2011] and the available seismic and geologic constraints on active faults in the Sunda-Banda Arc [*Hamilton*, 1979; *McCaffrey*, 1988]. We performed a simultaneous inversion of horizontal GPS velocities and earthquake slip vectors (supporting information Figure S1) to estimate Euler vectors of six blocks, locking depths at major Plate boundaries and three components of the strain rate tensor for three blocks (Sumba block, Timor block, and East Makassar block). The flexibility of this approach allows us to verify the significance and the importance of each plate boundary in the kinematic model. We have investigated the present-day deformation in this region using four kinematic models with different geometrical configurations of elastic blocks (Figure S5). Our preferred block model includes two major boundaries that encompass the Sunda-Banda Arc: the Java Trench and Timor Trough in the southern part and the back-arc thrusts system extending from the Wetar thrust to the Kendeng thrust east of Java island in the north. We divide the Arc into three blocks: The Timor Block [*McCaffrey*, 1988], Sumba Block, and the Eastern Java Block (Figure 3). In the southern part of Sulawesi, we divide the Makassar Block [*Socquet et al.*, 2006] into eastern and western blocks following the southern extension of the Walanae Fault and Selayar Trough [*Camplin and Hall*, 2014]. The boundary we use to separate the Banda Sea from the Weber Basin is speculative and may have a different geometry, though we do not currently have observations constraining its precise location. It is not specified as a fault and treated here as free-slipping boundary.

For the downdip geometry, the faults along the back-arc thrust are assigned a uniform dip angle of 30° in accordance with seismic reflection profiles [*Silver et al.*, 1983] and discretized with a 5 km downdip interval from the surface down to 30 km; however, the geometry of Java Trench and Timor Trough was based on the U.S. Geological Survey slab 1.0 [*Hayes et al.*, 2012] as well as on seismicity cross sections established across the main thrust for the eastern part were slab 1.0 model is not available. The nodes downdip are placed at depth every 2 km in the upper 10 km then every 5 km from 10 to 45 km depth and then every 10 km down to 70 km depth. In order to reduce the number of free parameters, we have estimated uniform locking depths at Wetar, Flores, Bali-Lombok, and Kendeng thrusts and we have parameterized the locking along the Java Trench as a function exponentially varying down depth while inverting for the minimum and maximum locking depths of the transition zone [*Wang et al.*, 2003; *McCaffrey et al.*, 2007]. The four plausible block model scenarios we investigate here include different combinations of block boundaries where seismicity or geologic constraints do not provide a unique solution for the surface expression of an active crustal fault. The assessment of the

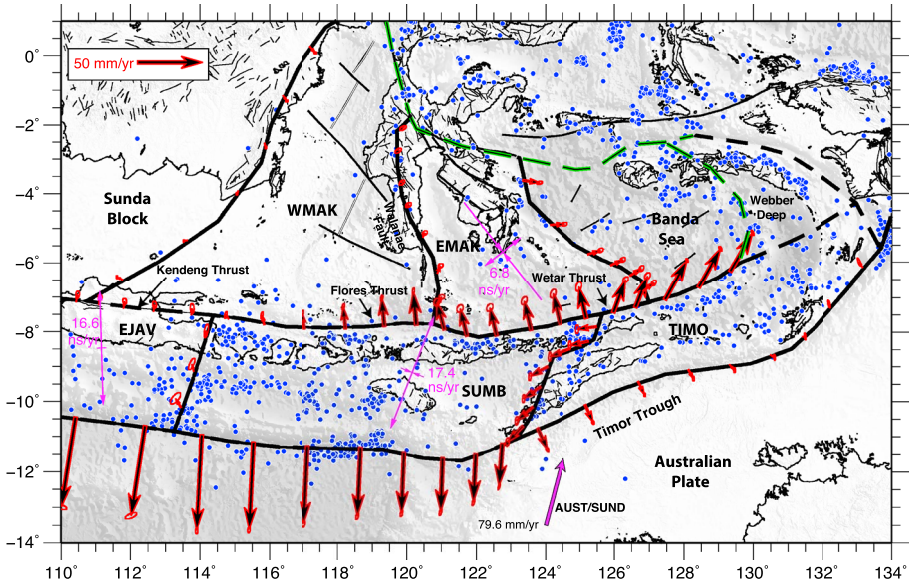

Figure 3. Relative slip vectors across block boundaries, derived from our best fit model. Arrows show motion of the hanging wall (moving block) relative to the footwall (fixed block) with 95% confidence ellipses. The tails of arrows is located within the "moving" block. Black thick lines show well-defined boundaries we use as active faults in our model and dashed lines show less well-defined boundaries (green : free-slipping boundaries and black: fixed locked faults) . Principal axes of the horizontal strain tensor estimated for the SUMB, EMAK, and EJAV are shown in pink. The thick pink arrow shows the relative motion of Australia with respect to Sunda (AUST/SUND). Abbreviations are Sumba Block (SUMB), West Makassar Block (WMAK), East Makassar Block (EMAK), East Java Block (EJAV), and Timor Block (TIMO). The background seismicity is from the International Seismological Centre catalog with magnitudes ≥ 5.5 and depths < 40 km.

significance of the geometrical complexity of alternate models was based on *F* test statistics. The detailed summary of the fit statistics is provided in the supporting information (Table S1).

3. GPS Velocity Field

The velocity field with respect to the Sunda Block (Figure 2a) reveals an anticlockwise rotation of the whole of eastern Sunda-Banda Arc with an increase in the motion of the archipelago from 9 mm/yr in Bali to 82 mm/yr toward the eastern end of the Timor Trough. This general increase in the northward velocity of the fore-arc is consistent with the convergence between the Australian Plate and the Sunda Block being progressively transferred north as the Australian Plate collision transitions from ocean arc in the West to continent-arc collision in the East. Motion decreases north of the back-arc toward south Sulawesi, reflecting the conclusions of previous studies that the back-arc is accommodating deformation [*McCaffrey*, 1988]. However, our new GPS data along East Java, Madura Island, and Bali Island reveal a significant north-south gradient of velocities across the Kendeng Basin and the volcanic arc (Figure 2b). This confirms that the boundary marking the transition from the Kendeng Basin to the Sunda shelf, known as the Kendeng thrust [*Smyth et al.*, 2008], is active and probably defines the westward onshore extension of the Flores back thrust [*Simandjuntak and Barber*, 1996].

Our kinematic model results show that the along-arc change in partitioning of plate convergence is caused by the anticlockwise rotation of the Sunda-Banda Arc with respect to Sunda Block. The relative motion, between the Asutralian Plate and the Sunda Block, along the Java Trench decreases from 70 ± 1.0 mm/yr west of the Lombok Basin (115°E) to 33 ± 0.9 mm/yr south of Rote Island (123°E) (Figure 3). Eastward of Timor Island (124°E), the relative motion along the Timor Trough gradually diminishes from 32 ± 2.0 mm/yr to an insignificant 1.0 ± 1.7 mm/yr at Tual Island (132°E). In contrast, the relative motion along the back-arc increases from west to east, from 6 ± 1.0 mm/yr in East Java to 26 ± 1.0 mm/yr at Flores, 28 ± 1.7 mm/yr at Wetar and 30 ± 1.8 mm/yr to the North of Timor, where the direction of vectors changes to more NE implying that a significant component of shearing must be accommodated by the structures at the back-arc in this area. This correlates well with the left-lateral strike-slip faulting inferred from the earthquake fault plane solutions (supporting information Table S2 and Figure S2).

4. Discussion and Implications for Earthquake Hazard

The description of the present-day motion within the eastern Sunda-Banda Arc is a debated question, with proposed models suggesting that the deformation can be described by several independent crustal blocks [*McCaffrey*, 1988; *Genrich et al.*, 1996] and others proposing this region as a wide zone of distributed deformation with diffuse transitional zones [*Nugroho et al.*, 2009]. Our results from the interpretation of the new GPS velocity field as well as the kinematic model suggest that the eastern Sunda-Banda is segmented into three blocks (East Java Block, Sumba Block, and Timor Block) separated by NE transitions of left-lateral faults. The Semau Fault (SF, Figure 1) is one of a series of NNE-SSW trending left-lateral strike-slip faults west of Timor [*Charlton et al.*, 1991] and may have been associated with a large earthquake in 1814 [*Soloviev and Go*, 1974]. Our best fit block model requires a boundary at the Semau Fault connecting the Timor Trough with the Wetar thrust, thus forming the western boundary of the Timor Block. The Semau Fault is a key component of our kinematic model as it provides the structural link between the fore-arc and the back-arc.

Our model requires the addition of a boundary approximately perpendicular to the Java Trench, allowing movement of this arc segment, known as the Sumba Block [*McCaffrey*, 1988], which is independent of the Java fore-arc. We chose the location of this fault where marine seismic and gravity modeling studies [*Shulgin et al.*, 2011] indicate fracturing in the upper 2 km of the oceanic crust and a sharp increase in crustal thickness. This fault accommodates only 3 to 4 mm/yr of strike-slip motion, less than 5% of the total relative motion, but its inclusion improves significantly the fit of the data (Table S1).

The northwestern corner of the Sumba Block abuts the offshore extension of the Kendeng thrust, where we estimate 5 ± 0.4 mm/yr of convergence. The presence of mud volcanoes [*Istadi et al.*, 2009] in the eastern part of the Kendeng Basin is consistent with overpressuring caused by active convergence in this area. Although some historical earthquakes may have occurred on the Kendeng thrust in the nineteenth century [*Simandjuntak and Barber*, 1996], the absence of more recent events raises the question of whether this fault is slipping aseismically or is fully locked. The current spatial resolution of the GPS network is insufficient to resolve the heterogeneity in the coupling on the back-arc thrusts. Therefore, we chose to estimate a uniform locking depth at each segment. On the Kendeng thrust, we estimated a locking depth of 9 ± 3 km and found that the segment north of Sumbawa Island is the deepest locked segment (20 ± 1.8 km) along the back-arc, with a moment deficit of 2.4×10^{18} Nm, equivalent approximately to an earthquake of magnitude $M_w = 6.3$. Between 2006 and 2009 a sequence of 3 earthquakes with $M_w > 6.3$ occurred in the eastern part of this segment at depths ranging between 18 and 20 km. A recent study [*Fuchs et al.*, 2014] detected the occurrence of triggered nonvolcanic tremors beneath Sumbawa Island, which might increase the recurrence time of major events ($> M_w 7$) by helping to release strain during the interseismic period.

In contrast to the localization of deformation in the Sunda-Banda back-arc at the Flores and Wetar thrusts inferred by previous studies, we find that active deformation extends along the back-arc for over ~2000 km. This accounts for a variation from 5% to 40% of the total convergence between the Australian Plate and the Sunda Block and explains the distribution of both historical and recorded seismic events. Our results elucidate the role of the left-lateral Semau Fault west of Timor in transferring the shear stress from the trench to the back-arc (Figure 4), where NE shearing at 20 mm/yr predominates along the transfer boundary with a normal convergence component of 4 to 9 mm/yr on this fault. This shear zone also marks a transition where the convergence obliquity along the back-arc changes from normal at Flores (5°N) to a more oblique direction along east Wetar (17°N), consistent with the difference in shortening [*Silver et al.*, 1983] observed on the Wetar (~10 km) and Flores (~30 km) thrusts. This suggests that the increase of stress due to the obliquity reflects a recent evolutionary stage of underthrusting across the Wetar back-arc segment migrating eastward.

The concept of slip partitioning in obliquely convergent fault systems is used to explain the accommodation of shear strain resulting from the trench-parallel component of the relative motion [*Fitch*, 1972]. The classic model requires the megathrust plate boundary to accommodate the trench-normal slip, and a parallel strike-slip fault in the fore-arc to take up the oblique slip, with both structures isolating a continental wedge known as a sliver [*Fitch*, 1972; *McCaffrey*, 1988]. Along the transition from the eastern Java Trench to Timor Trough, the direction of the plate convergence becomes progressively oblique to the east, where earthquake slip vectors show a complex pattern of deformation typical of highly curved margins as documented by *McCaffrey* [1996]. Previous studies demonstrated that the degree of the deformation partitioning is a function of the convergence obliquity [*McCaffrey*, 1992; *Vernant and Chéry*, 2006]. However, they showed that full partitioning is reached only for high-obliquity values larger than ~70°. In our study we predict that only

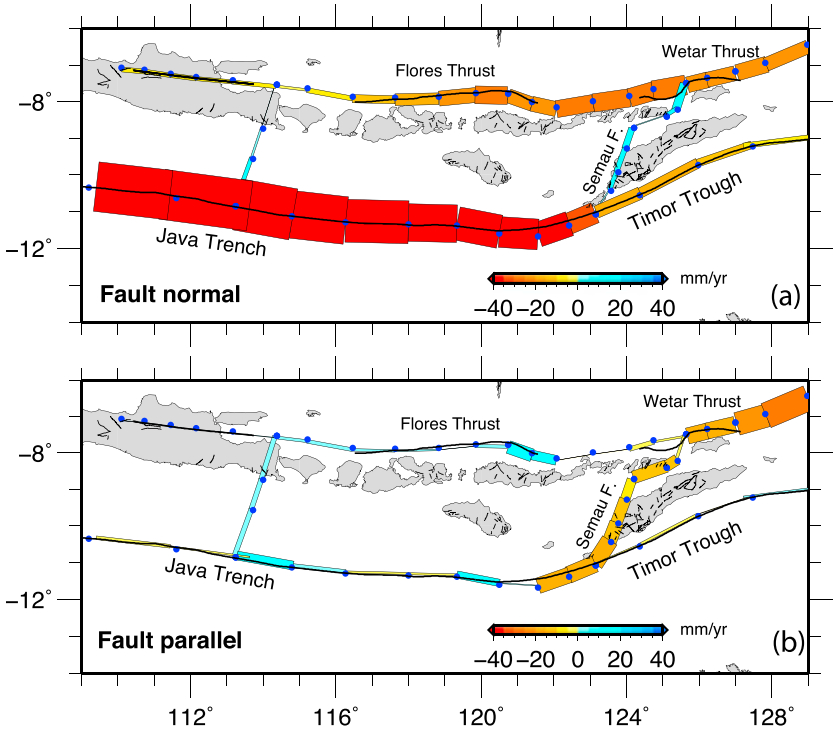

Figure 4. Fault slip rate components: (a) fault normal (extension positive) and (b) fault parallel (right-lateral positive).

~37% of the total lateral shear strain is accommodated on Timor Trough and the back-arc thrusts to the north, suggesting that full partitioning is less likely to occur, consistent with 3-D mechanical modeling predictions [*Vernant and Chéry*, 2006]. However, it is unclear how the remaining unaccounted deformation is accommodated and we speculate it is likely to be partitioned further north on the Seram Trough, where the analysis of focal mechanisms show signs of active deformation. Quantifying precisely where and how this remaining motion is accommodated is beyond the scope of this paper requiring more dense GPS observations in the north Banda Sea region.

Our results show a different structural organization, where the convergence itself is transferred to the back-arc. As with classical slip partitioning, this results in isolation of an arc segment (the Sumba Block), and partitioning of convergence is achieved through a combination of anticlockwise rotation of the Sumba fore-arc Block and left-lateral movement along the Semau Fault (Figure 4). A similar organization is observed elsewhere in the world where back-arc thrusting is active, such as the great Antilles Arc [*Mann et al.*, 2002], the North Panama Deformed belt [*Kobayashi et al.*, 2014] and the New Hebrides/Vanuatu [*Calmant et al.*, 2003]. These zones of back-arc thrusting are approximately 500 km, 600 km, and 200 km, respectively, in length. Our results show a far more extensive zone of active thrusting along a ~2000 km section of the eastern Sunda Arc, a potentially important source of seismic and tsunami hazard.

5. Conclusion

Our results draw a new kinematic framework for active deformation in the eastern Sunda-Banda Arc, highlighting the need to reconsider the level of seismic hazard there. Several of the active faults identified here directly threaten socioeconomic assets vital to Indonesia. The Kendeng thrust passes through the southern outskirts of Surbaya, Indonesia's second largest city with a population of over 2.5 million, and traverses a 300 km length of East Java, with a population density of over 800 people per square kilometer. The Semau Fault skirts the city of Kupang, the main commercial centre of Nusa Tenggara with a population of around 500,000. Finally, earthquakes along the back-arc thrust beneath the sea floor extending 1700 km from eastern Java to Timor could generate regional tsunamis threatening the coastlines of the Flores Sea. Further studies, including earthquake, geodetic, and paleoseismic, should be undertaken to better understand these threats.

Acknowledgments
This research was supported under the Australian Research Council's Linkage Projects funding scheme (LP110100525). Figures are drawn with GMT [*Wessel and Smith*, 1998]. The GPS data were computed on the Terrawulf II computational facility at the Research School of Earth Sciences, a facility supported through the AuScope initiative. AuScope Ltd is funded under the National Collaborative Research Infrastructure Strategy (NCRIS), an Australian Commonwealth Government Program. We are grateful to Nyamadi, Dodi Sudarmono, Caca Juniarsa, Budi Parjanto, Heru derajat, Sidik Tri Wibowo, Munawar Kholil and Putra Maulida, and all to the personnel of Badan Informasi Geospatial (BIG), who participated in GPS surveys over the past 20 years. We appreciate constructive comments and improvements from two anonymous reviewers.

References

Beckers, J., and T. Lay (1995), Very broadband seismic analysis of the 1992 Flores, Indonesia, earthquake (M_w = 7.9), *J. Geophys. Res.*, *100*(B9), 18,179–18,193, doi:10.1029/95JB01689.

Bock, Y., L. Prawirodirdjo, J. F. Genrich, C. W. Stevens, R. McCaffrey, C. Subarya, S. S. O. Puntodewo, and E. Calais (2003), Crustal motion in Indonesia from Global Positioning System measurements, *J. Geophys. Res.*, *108*, 2367, doi:10.1029/2001JB000324.

Calmant, S., B. Pelletier, P. Lebellegard, M. Bevis, F. W. Taylor, and D. A. Phillips (2003), New insights on the tectonics along the New Hebrides subduction zone based on GPS results, *J. Geophys. Res.*, *108*, 2319, doi:10.1029/2001JB000644.

Camplin, D. J., and R. Hall (2014), Neogene history of Bone Gulf, Sulawesi, Indonesia, *Mar. Petrol. Geol.*, *57*, 88–108.

Charlton, T. R., A. J. Barber, and S. T. Barkham (1991), The structural evolution of the Timor collision complex, eastern Indonesia, *J. Struct. Geol.*, *13*, 489–500.

Ekström, G., M. Nettles, and A. M. Dziewonski (2012), The global CMT project 2004–2010: Centroid-moment tensors for 13,017 earthquakes, *Phys. Earth Planet Inter.*, *1–9*, 200–201.

Feng, L., E. M. Hill, P. Banerjee, I. Hermawan, L. L. H. Tsang, D. H. Natawidjaja, B. W. Suwargadi, and K. Sieh (2015), A unified GPS-based earthquake catalog for the Sumatran plate boundary between 2002 and 2013, *J. Geophys. Res. Solid Earth*, *120*, 3566–3598, doi:10.1002/2014JB011661.

Fitch, T. J. (1972), Plate convergence, transcurrent faults, and internal deformation adjacent to Southeast Asia and the western Pacific, *J. Geophys. Res.*, *77*(23), 4432–4460, doi:10.1029/JB077i023p04432.

Fuchs, F., M. Lupi, and S. A. Miller (2014), Remotely triggered nonvolcanic tremor in Sumbawa, Indonesia, *Geophys. Res. Lett.*, *41*, 4185–4193, doi:10.1002/2014GL060312.

Genrich, J. F., Y. Bock, R. McCaffrey, E. Calais, C. W. Stevens, and C. Subarya (1996), Accretion of the southern Banda arc to the Australian plate margin determined by Global Positioning System measurements, *Tectonics*, *15*(2), 288–295, doi:10.1029/95TC03850.

Hamilton, W. B. (1979), Tectonics of the Indonesian region, *Tech. Rep. No. 1078*, U.S. Govt. Print. Off., Wash.

Hayes, G. P., D. J. Wald, and R. L. Johnson (2012), Slab1.0: A three-dimensional model of global subduction zone geometries, *J. Geophys. Res.*, *117*, B01302, doi:10.1029/2011JB008524.

Herring, T. A., R. W. King, and S. C. McClusky (2010), *Introduction to GAMIT/GLOBK*, Mass. Inst. of Tech., Cambridge.

Istadi, B. P., G. H. Pramono, P. Sumintadireja, and S. Alam (2009), Modeling study of growth and potential geohazard for LUSI mud volcano: East Java, Indonesia, *Mar. Petrol. Geol.*, *26*(9), 1724–1739.

Kobayashi, D., P. LaFemina, H. Geirsson, E. Chichaco, A. A. Abrego, H. Mora, and E. Camacho (2014), Kinematics of the western Caribbean: Collision of the Cocos Ridge and upper plate deformation, *Geochem. Geophys. Geosyst.*, *15*, 1671–1683, doi:10.1002/2014GC005234.

Mann, P., E. Calais, J.-C. Ruegg, C. DeMets, P. E. Jansma, and G. S. Mattioli (2002), Oblique collision in the northeastern Caribbean from GPS measurements and geological observations, *Tectonics*, *21*(6), 1057, doi:10.1029/2001TC001304.

McCaffrey, R. (1988), Active tectonics of the Eastern Sunda and Banda Arcs, *J. Geophys. Res.*, *93*(B12), 15163–15182, doi:10.1029/JB093iB12p15163.

McCaffrey, R. (1992), Oblique plate convergence, slip vectors, and forearc deformation, *J. Geophys. Res.*, *97*, 8905–8915.

McCaffrey, R. (1996), Slip partitioning at convergent plate boundaries of SE Asia, in Tectonic Evolution of SE Asia Symposium, *Geol. Soc. Spec. Publ.*, *106*, 3–18.

McCaffrey, R. (2005), Block kinematics of the Pacific-North America plate boundary in the southwestern United States from inversion of GPS, seismological, and geologic data, *J. Geophys. Res.*, *110*, B07401, doi:10.1029/2004JB003307.

McCaffrey, R., A. I. Qamar, R. W. King, R. Wells, G. Khazaradze, C. A. Williams, C. W. Stevens, J. J. Vollick, and P. C. Zwick (2007), Fault locking, block rotation and crustal deformation in the Pacific Northwest, *Geophys. J. Int.*, *169*, 1315–1340, doi:10.1111/j.1365-246X.2007.03371.x.

Musson, R. M. W. (2012), A provisional catalogue of historical earthquakes in Indonesia, *Open Report OR/12/073*, pp. 21, Geological Survey, Edinburgh, British.

Nugroho, H., R. Harris, A. W. Lestariya, and B. Maruf (2009), Plate boundary reorganization in the active Banda Arc-continent collision: Insights from new GPS measurements, *Tectonophysics*, *479*, 52–65, doi:10.1016/j.tecto.2009.01.026.

Reilinger, R., et al. (2006), GPS constraints on continental deformation in the Africa-Arabia-Eurasia continental collision zone and implications for the dynamics of plate interactions, *J. Geophys. Res.*, *111*, B05411, doi:10.1029/2005JB004051.

Silver, E. A., D. Reed, R. McCaffrey, and Y. Joyodiwiryo (1983), Back-arc thrusting in the Eastern Sunda Arc Indonesia: A consequence of arc-continent collision, *J. Geophys. Res.*, *88*(B9), 7429–7448, doi:10.1029/JB088iB09p07429.

Simandjuntak, T. O., and A. J. Barber (1996), Contrasting tectonic styles in the Neogene orogenic belts of Indonesia, *Geol. Soc. Spec. Publ.*, *106*(1), 185–201.

Shulgin, A., H. Kopp, C. Mueller, L. Planert, E. Lueschen, E. R. Flueh, and Y. Djajadihardja (2011), Structural architecture of oceanic plateau subduction offshore Eastern Java and the potential implications for geohazards, *Geophys. J. Int.*, *184*, 12–28, doi:10.1111/j.1365-246X.2010.04834.x.

Smyth, H. R., R. Hall, and G. J. Nichols (2008), Cenozoic volcanic Arc history of east Java, Indonesia: The stratigraphic record of eruptions on an active continental margin, *Geol. Soc. Am. Spec. Pap.*, *436*, 199–222.

Socquet, A., W. Simons, C. Vigny, R. McCaffrey, C. Subarya, D. Sarsito, B. Ambrosius, and W. Spakman (2006), Microblock rotations and fault coupling in SE Asia triple junction (Sulawesi, Indonesia) from GPS and earthquake slip vector data, *J. Geophys. Res.*, *111*, B08409, doi:10.1029/2005JB003963.

Soloviev, S. L., and Ch. N. Go (1974), *A Catalogue of Tsunamis on the Western Shore of the Pacific Ocean*, pp 308, Nauka Publishing House, Moscow.

Vernant, P., and J. Chéry (2006), Mechanical modelling of oblique convergence in the Zagros Iran, *Geophys. J. Int.*, *165*, 991–1002.

Vigny, C., et al. (2005), Insight into the 2004 Sumatra-Andaman earthquake from GPS measurements in Southeast Asia, *Nature*, *436*, 201–206.

Wang, K., R. Wells, S. Mazzotti, R. D. Hyndman, and T. Sagiya (2003), A revised dislocation model of interseismic deformation of the Cascadia subduction zone, *J. Geophys. Res.*, *108*, 2026, doi:10.1029/2001JB001227.

Wessel, P., and W. H. F. Smith (1998), New, improved version of the genericmapping tools released, *Eos. Trans. AGU*, *79*, 579, doi:10.1029/98EO00426.